Polymer-coated bioactive glass S53P4 increases VEGF and TNF expression in an induced membrane model in vivo

Björkenheim, Robert

2017-08

Björkenheim , R , Stromberg , G , Pajarinen , J , Ainola , M , Uppstu , P , Hupa , L , Bohling , T O & Lindfors , N C 2017 , ' Polymer-coated bioactive glass S53P4 increases VEGF and TNF expression in an induced membrane model in vivo ' , Journal of Materials Science , vol. 52 , no. 15 , pp. 9055-9065 . https://doi.org/10.1007/s10853-017-0839-6

http://hdl.handle.net/10138/237056
https://doi.org/10.1007/s10853-017-0839-6

publishedVersion

J Mater Sci (2017) 52:9055–9065

In Honor of Larry Hench

Polymer-coated bioactive glass S53P4 increases VEGF and TNF expression in an induced membrane model in vivo

R. Björkenheim[1,2,9,*], G. Strömberg[1,2], J. Pajarinen[3], M. Ainola[2,4], P. Uppstu[5], L. Hupa[6], T. O. Böhling[7,8], and N. C. Lindfors[1,2]

[1] *Department of Musculoskeletal and Plastic Surgery, University of Helsinki, Helsinki, Finland*
[2] *Helsinki University Central Hospital, Helsinki, Finland*
[3] *Orthopaedic Research Laboratories, Department of Orthopaedic Surgery, Stanford University School of Medicine, Stanford, CA, USA*
[4] *Department of Medicine, Clinicum, University of Helsinki, Helsinki, Finland*
[5] *Laboratory of Polymer Technology, Centre of Excellence in Functional Materials at Biological Interfaces, Åbo Akademi University, Turku, Finland*
[6] *Johan Gadolin Process Chemistry Centre, Åbo Akademi University, Turku, Finland*
[7] *Department of Pathology, HUSLAB, Helsinki, Finland*
[8] *University of Helsinki, Helsinki, Finland*
[9] *Töölö Hospital, Topeliuksenkatu 5, 00260 Helsinki, Finland*

Received: 30 September 2016
Accepted: 24 January 2017
Published online: 2 February 2017

ABSTRACT

The two-stage induced-membrane technique for treatment of large bone defects has become popular among orthopedic surgeons. In the first operation, the bone defect is filled with poly(methyl methacrylate) (PMMA), which is intended to produce a membrane around the implant. In the second operation, PMMA is replaced with autograft or allograft bone. Bioactive glasses (BAGs) are bone substitutes with bone-stimulating and angiogenetic properties. The aim of our study was to evaluate the inductive vascular capacity of BAG-S53P4 and poly(lactide-co-glycolide) (PLGA)-coated BAG-S53P4 for potential use as bone substitutes in a single-stage induced-membrane technique. Sintered porous rods of BAG-S53P4, PLGA-coated BAG-S53P4 and PMMA were implanted in the femur of 36 rabbits for 2, 4 and 8 weeks. The expression of vascular endothelial growth factor (VEGF) and tumor necrosis factor alpha (TNF) in the induced membranes of implanted materials was analyzed with real-time quantitative polymerase chain reaction and compared with histology. Both uncoated BAG-S53P4 and PLGA-coated BAG-S53P4 increase expression of VEGF and TNF, resulting in higher amounts of capillary beds, compared with the lower expression of VEGF and less capillary beads observed for negative control and

R. Björkenheim and G. Strömberg have contributed equally to this work.

Address correspondence to E-mail: robert.bjorkenheim@hus.fi

DOI 10.1007/s10853-017-0839-6

PMMA samples. A significantly higher expression of VEGF was observed for PLGA-coated BAG-S53P4 than for PMMA at 8 weeks ($p < 0.036$). VEGF and TNF expression in the induced membrane of BAG-S53P4 and PLGA-coated BAG-S53P4 is equal or superior to PMMA, the "gold standard" material used in the induced-membrane technique. Furthermore, the VEGF and TNF expression for PLGA-coated BAG-S53P4 increased during follow-up.

Introduction

Treatment of bone defects, especially diaphyseal bone defects, is still a major clinical challenge usually requiring transplantation of autologous or allograft bone. Although autograft bone is one of the most commonly transplanted tissues and the gold standard in bone tissue reconstruction, it has disadvantages such as limited supply especially in children and elderly patients. Bone harvesting may also result in considerable donor site morbidity. Allograft bone is abundantly available, but has its own limitations, e.g., possible transmission of bacterial species [1].

Angiogenesis, including growth of blood vessels from preexisting vessels, is a prerequisite for bone formation. It is a complex phenomenon involving oxygen and several cell types, such as mature and progenitor endothelial cells, leukocytes and platelets, as well as growth factors [2]. Vascular endothelial growth factor (VEGF) is a multi-tasking cytokine that is known to play a central role both in angiogenesis and in fracture healing. It has also been suggested to participate in the treatment of critical size defects by increasing mineralization of the regenerated bone [3].

In 2000, Masquelet et al. [4] introduced a two-stage technique for the treatment of diaphyseal bone defects, which combines an induced-membrane technique with the use of cancellous autografts. In the first procedure, a poly(methyl methacrylate) (PMMA) spacer is inserted into the bone defect. After the insertion, a pseudo-synovial membrane will develop around the spacer. During the second operation, the spacer is removed and the defect is reconstructed using autologous cancellous bone grafts. The induced membrane is known to express various cytokines and growth factors supporting bone formation such as VEGF and tumor necrosis factor alpha (TNF). The production of these factors and the effectiveness of the induced membrane to support bone regeneration have, however, been observed to continuously diminish with time [5, 6].

Hench and Paschall [7] were the first to discover the group of synthetic silica-based BAGs with bone bonding properties in the late 1960s. Today, BAGs are used as bone substitutes providing osteoconductive and osteostimulative properties. These characteristics are known to depend on controlled dissolution and precipitation processes at the surface of the glass starting immediately after implantation. The reaction events commence with a rapid ion exchange of alkalis at the glass surface to hydrogen ions in the solution followed by dissolution and repolymerization of soluble silica. Finally calcium phosphate nucleates and crystallizes to hydroxyapatite at the surface of the glass [8]. The surface reactions give rise to an elevated pH of the solution in the interface between the implant and tissue, which partly explains the antibacterial properties observed for BAGs [9, 10].

Poly(α-hydroxy)acids such as polylactide (PLA), polyglycolide (PGA) and poly(lactide-co-glycolide) (PLGA) are commonly studied for applications in bone regeneration. During their degradation process, acidic products are released, with a subsequent decrease in pH in the vicinity of the implanted material, which may give rise to an inflammatory response. However, many degradable polymers have poor or lacking osteogenic and angiogenic activity. By combining BAGs and degradable polymers as composites, it was hypothesized that beneficial properties from both materials can be utilized to optimize the formation of an induced membrane and subsequent bone regeneration.

The aim of this study was to evaluate the vascular expression in a membrane induced by BAG or PLGA-coated BAG, compared with a PMMA spacer or a trauma (control) in an in vivo rabbit model.

Materials and methods

Bioactive glass

BAG-S53P4, with a wt% composition of 53% SiO_2, 23% NaO, 20% CaO and 4% P_2O_5, was made from mixtures of Belgian sand for SiO_2 and analytical grades of Na_2CO_3, $CaCO_3$ and $CaHPO_4{\cdot}2H_2O$. The glass was melted in a platinum crucible for 3 h at 1360 °C. After casting in a preheated graphite mold, the glass was crushed and re-melted for homogenization. Annealed glass blocks were crushed and sieved to a size range fraction of 300–500 μm. The glass particles were sintered in graphite molds at 720 °C in nitrogen atmosphere for 90 min to cylindrical rods with the length of 15 mm and a diameter of 5 mm.

Polymer coating

An acid-terminated poly(DL-lactide-co-glycolide) (PLGA) named PDLG5002A with a 50/50 ratio between DL-lactide and glycolide (Corbion, Gorinchem, the Netherlands) was used for coating one end of the sintered BAG rods. The coating was carried out by immersing approximately 2 mm of the end of the BAG implant, in a dichloromethane solution containing 20 wt% PLGA. The partly coated BAG-S53P4-PLGA implants were thereafter dried in air and vacuum. The implants were gamma-sterilized with a dose of 25 kGy.

Poly(methyl methacrylate), PMMA

Commercially available PMMA bone cement Palacos + G (Heraeus Medical GmbH, Wehrheim, Germany) was mixed according to the manufacturer's instructions. PMMA rods with a length of 15 mm and a diameter of 5 mm size were made under sterile conditions and sterilized in an autoclave oven prior to animal surgery.

Animals and surgery

Thirty-six skeletally mature rabbits (NZW, Harlan Laboratories) were used. The animal study was approved by the Animal Experimental Board of Finland (ESAVI/440/04.10.07/2014), and the principles of laboratory animal care of the University of Helsinki were strictly followed.

The operations were performed under general anesthesia using subcutaneous medetomidine hydrochloride and ketamine hydrochloride. A bone defect was performed by drilling a 6-mm horizontal hole from the lateral to the medial part of the distal metaphyseal region of the femur. One 5 × 15 mm rod of either BAG-S53P4, BAG-S53P4-PLGA or PMMA was implanted in the created bone defect. The BAG-S53P4-PLGA rods were implanted placing the coated end in the cortical region of the bone against soft tissue. Three parallel experiments for each combination of rod and time point were used. Three defects per time point were left empty for control. Cefuroxime, buprenorphine and carprofen were given for 3 days postoperatively to prevent infections and to relieve pain. Postoperatively at 2, 4 and 8 weeks, the animals were euthanized with an overdose of pentobarbital. The membranes induced at the end of the implants as well as at the site of the control hole were collected. For histochemistry, the samples were stored in 10% formalin overnight, then washed and stored in 70% EtOH to be further processed. Samples for real-time quantitative polymerase chain reaction (RT-qPCR) analysis were stored in RNA later solution (AM7020) at 4 °C overnight and then stored in sterile tubes at −80 °C to await further processing.

Real-time quantitative polymerase chain reaction (RT-qPCR)

Induced-membrane tissue samples of 30–50 mg were homogenized in Trizol solution (Invitrogen/Life Technologies Paisley, UK) with an Ultra-Turrax homogenizer. Upper aqueous layer containing RNA was separated by centrifugation with chloroform and combined with the RNeasy Mini Kit (Qiagen, Valencia, CA, USA) for total RNA isolation according to the manufacturer's instructions. cDNA was synthesized from 600 ng of isolated RNA using an iScript cDNA synthesis kit (Bio-Rad, Hercules, CA, USA) and diluted 1:3 with RNA-free water. cDNA synthesis was performed two separate times from the same total RNA samples, and qPCR was performed twice for both samples using iQ5 real-time PCR detection system (Bio-Rad). The reaction mixture for qPCR was 10 μl of iQ SYBR green, 7 μl of water, 2 μl of cDNA (20 ng) and 1 μl of 5 μM primers. The primer sequences were as follows; VEGF (247 bp; Acc

no. AY196796): sense 5′-CACCCATGGCAGAAGAAGGA-3′, antisense 5′-ATCCGCATGATCTGCATGGT-3′ and for TNF (281 bp; Acc no. NM_001082263): sense 5′-GAGTCCCCAAACAACCTCCA-3′, antisense 5′-TGAGTGAGGAGCACGTAGGA-3′. As a reference gene, GAPDH (207 bp; Acc no. NM_001082253) was used with the following sequence: sense 5′-CGAGCTGAACGGGAAACTCA-3′, antisense 5′-TGGGTGGCACTGTTGAAGTC-3′. Results were calculated with Gene Expression Macro for Microsoft Excel, version 1.1 (Bio-Rad).

Hematoxylin and eosin staining

Samples of the induced membrane were after harvesting fixated in 10% formalin overnight for hematoxylin and eosin (H&E) staining. The samples were processed with KOS multifunctional microwave tissue processor (Milestone Srl, Sorisole BG, Italy), embedded in paraffin with Microm EC 350 Tissue Embedding Center (Thermo Scientific, Kalamazoo, MI, USA) for producing paraffin blocks and cut into 3-μm sections using RM 2255 Microtome (Leica Microsystems, Wetzlar, Germany). Tissue sections were deparaffinized in xylene and hydrated through a descending alcohol series to water using automatic stainer (Varistain XY, Shandon, Life Sciences International LTD, Cheshire, England). This was followed by 10-min incubation in hematoxylin to stain cell nuclei and 5 min in 0.5% eosin to stain cytoplasm and extracellular matrix, and dehydrated in an ascending alcohol series, cleared in xylene and mounted.

The H&E stained sections were evaluated for the presence of capillary beds using a Leica DM6000 B/M light microscope connected to a digital camera (DFC420 and DFC365FX; Leica Microsystems). Images with 10× magnifications were obtained from each sample and time point. In order to get the best result for each type of membrane, one representative sample from each treatment group and time point was selected and a manual capillary vessel count was preformed from three different regions with the most capillaries seen located in the surrounding of the lining of the membrane using ImageJ software (version 2.0.0-rc-43/1.51h, open-source image processing software). This was done because there were apparent differences in the quality of samples, even between membranes of the same type and time point.

Statistical analysis

One rabbit deceased 3 days after the surgical procedure from diarrhea for an unknown reason, resulting in duplicate samples for PMMA at 2 weeks compared to triplicates for BAG-S53P4 and BAG-S53P4-PLGA. One-way ANOVA analysis followed by Tukey's multiple comparison post hoc follow-up test was used to calculate statistical differences using Prism software (version 7.0a, GraphPad Software, Inc.). $p < 0.05$ was chosen as the threshold of statistical significance.

Results

Real-time quantitative polymerase chain reaction (RT-qPCR)

A high expression of VEGF for the control membrane was observed at 2 weeks, but the expression levels rapidly declined, not being applicable for analysis at 8 weeks. This was in contrast to the PMMA treated group, for which a low but only slightly decreasing expression of VEGF was observed up to 8 weeks. The VEGF expression for the uncoated BAG-S53P4 induced membranes was highly up-regulated at 2 weeks being significantly higher compared to PMMA ($p = 0.043$) and PLGA-coated BAG-S53P4 ($p = 0.018$), but declined to the level for PMMA and coated BAG-S53P4 at the 4-week time point. Interestingly, the PLGA-coated BAG-S53P4 changed the pattern of VEGF expression and, rather than declining over time, a steady increase from low to high VEGF expression over the 8-week period could be observed being significantly higher at the 8-week time point compared to the 2-week time point ($p = 0048$). Furthermore, at 8 weeks, the VEGF expression in PLGA-coated BAG-S53P4 samples was significantly higher than in PMMA membranes ($p = 0036$). While the difference in VEGF expression between PLGA-coated BAG-S53P4 and uncoated BAG-S53P4 membranes was apparent, it did not reach statistical significance. However, a clear trend for statistical significance was observed ($p = 0066$) between BAG-S53P4-PLGA and BAG-S53P4 at the 8-week time point.

The TNF expression for the control drill samples was low throughout the follow-up, being inadequate for analysis at 8 weeks. The TNF expression for

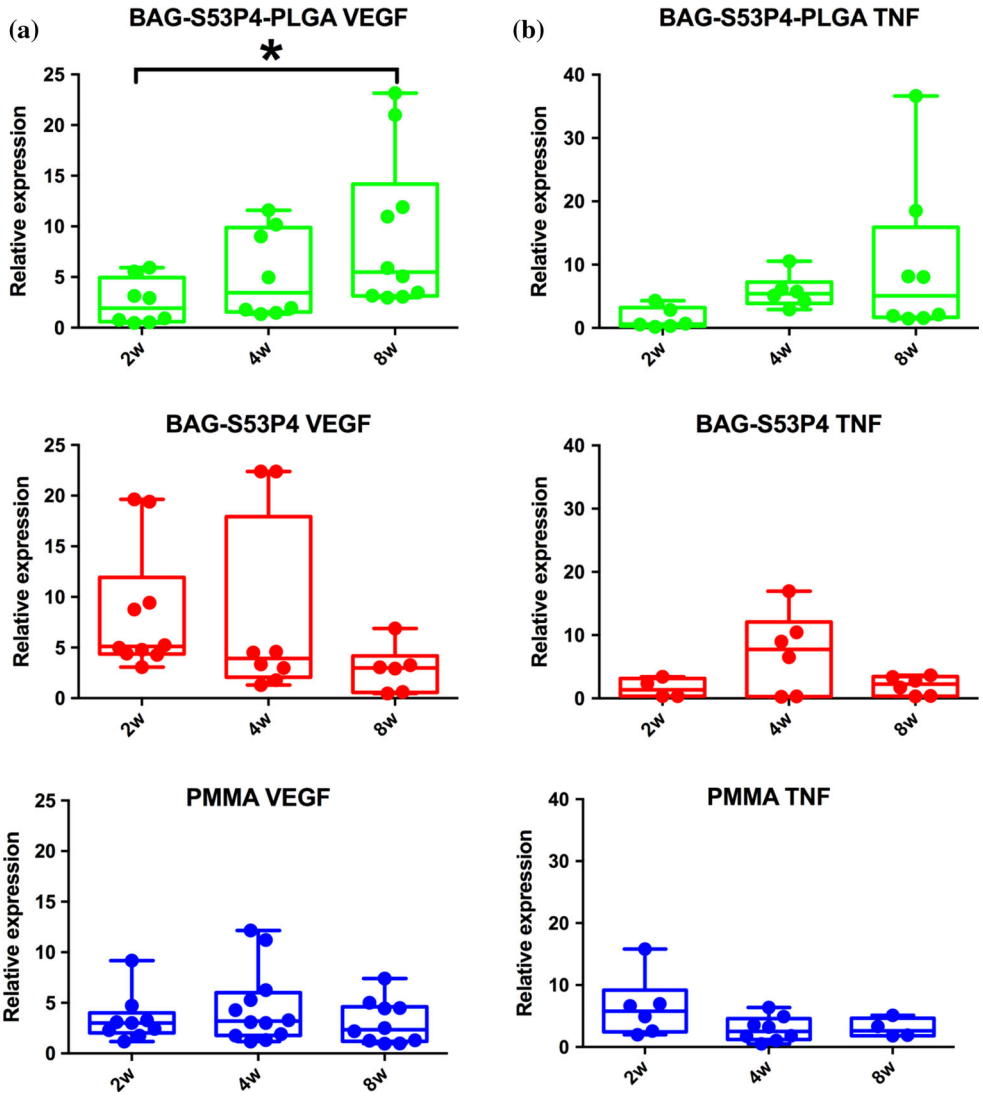

Figure 1 VEGF (**a**) and TNF (**b**) relative expression levels over time in BAG-S53P4-PLGA, BAG-S53P4 and PMMA-induced membrane tissue samples. *Box* showing median with interquartile range, *bars* showing min to max; * statistical significance $p < 0.05$.

PMMA reached its peak at 2 weeks and was apparently higher compared to uncoated and coated BAG-S53P4, with a declining trend toward the end of the follow-up. At this 2-week time point, PMMA showed a trend for statistical significance when compared to BAG-S53P4-PLGA ($p = 0056$). This was in contrast to the PLGA-coated BAG-S53P4, for which an increase in TNF expression, consistent with the VEGF expression pattern for PLGA-coated BAG-S53P4, was observed throughout the follow-up.

The results of qPCR are summarized in Figs. 1 and 2.

Histology

A high presence of capillary beds was observed at 2 weeks in the control drill membrane specimens. The number declined during follow-up and at 8 weeks only few capillary beds were observed ($p = 0.014$). The PMMA-induced membrane showed a stable capillary count at every time point, although with a declining trend. The BAG-S53P4-induced membrane had a clear peak of capillary bed density at 2 weeks, which declined to the level of the PMMA-induced membrane at 4- and 8-week time point. Comparing the different membranes of BAG-S53P4, the 2-week induced membrane had significantly more capillaries than the 4-week ($p = 0.025$) and the 8-week ($p = 0.035$) induced membranes. The BAG-S53P4-PLGA membranes were similar to the PMMA at the 2-week time point. However, at 8 weeks the BAG-S53P4-PLGA-induced membrane had clearly the highest number of capillary vessels compared to all other induced membranes. This observation was

statistically significant for the control membrane ($p = 0.0058$) and PMMA membrane ($p = 0.045$). These results are shown in Fig. 3. The 8-week H&E stains for each type of induced membrane are shown in Fig. 4a–d.

Figure 3 The capillary vessel count results at different time points from most representative control membrane tissue sample and BAG-S53P4-PLGA, BAG-S53P4 and PMMA-induced membrane tissue samples. *Bars* show mean SEM. **a** Illustration of capillary count at different time points. **b** Illustrates the capillary count from the three regions of the same sample separately over time.

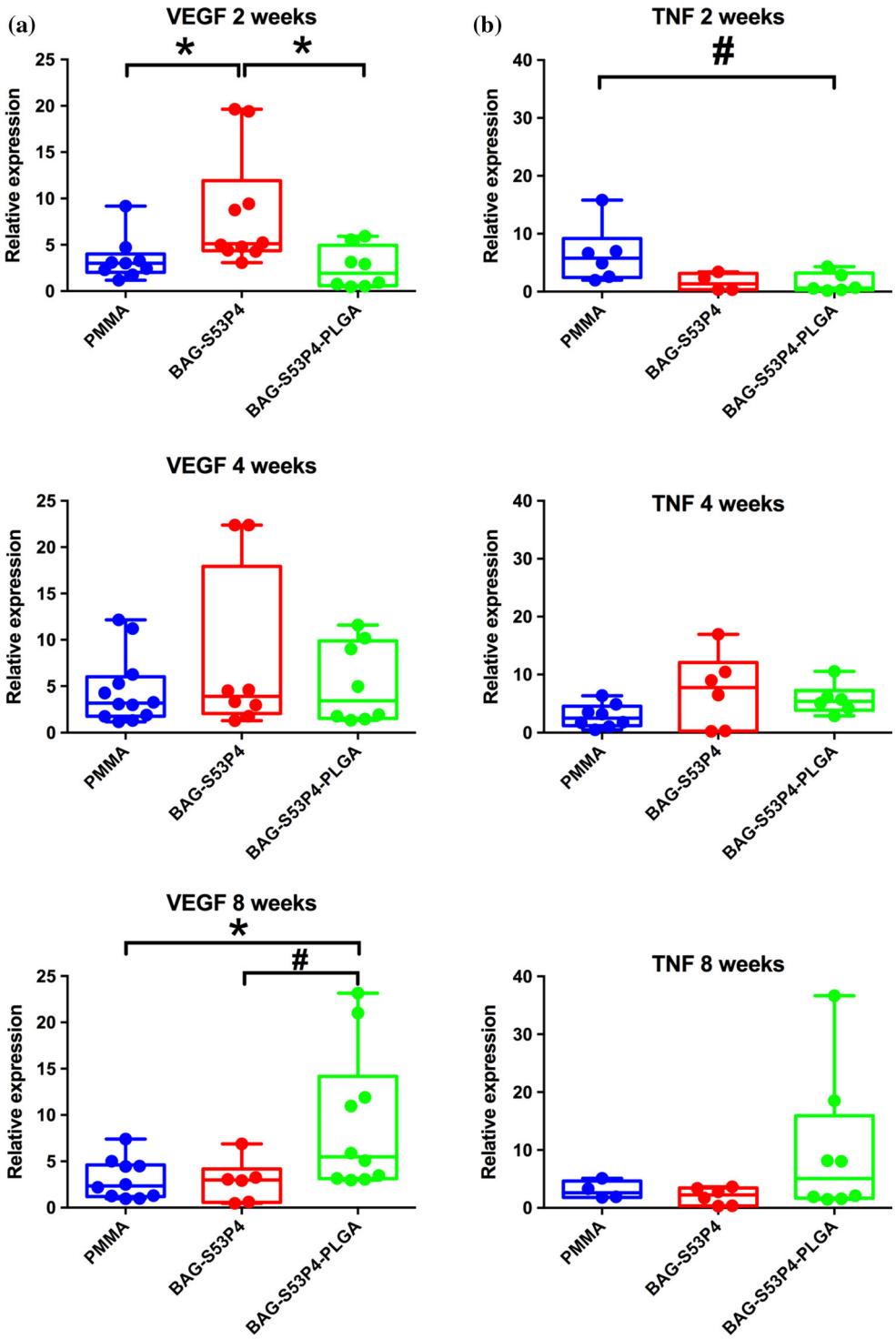

Figure 2 VEGF (**a**) and TNF (**b**) relative expression levels at specific time points in BAG-S53P4-PLGA, BAG-S53P4 and PMMA-induced membrane tissue samples. *Box* showing median with interquartile range, *bars* showing min to max; * statistical significance $p < 0.05$; # statistical trend $p < 0.07$.

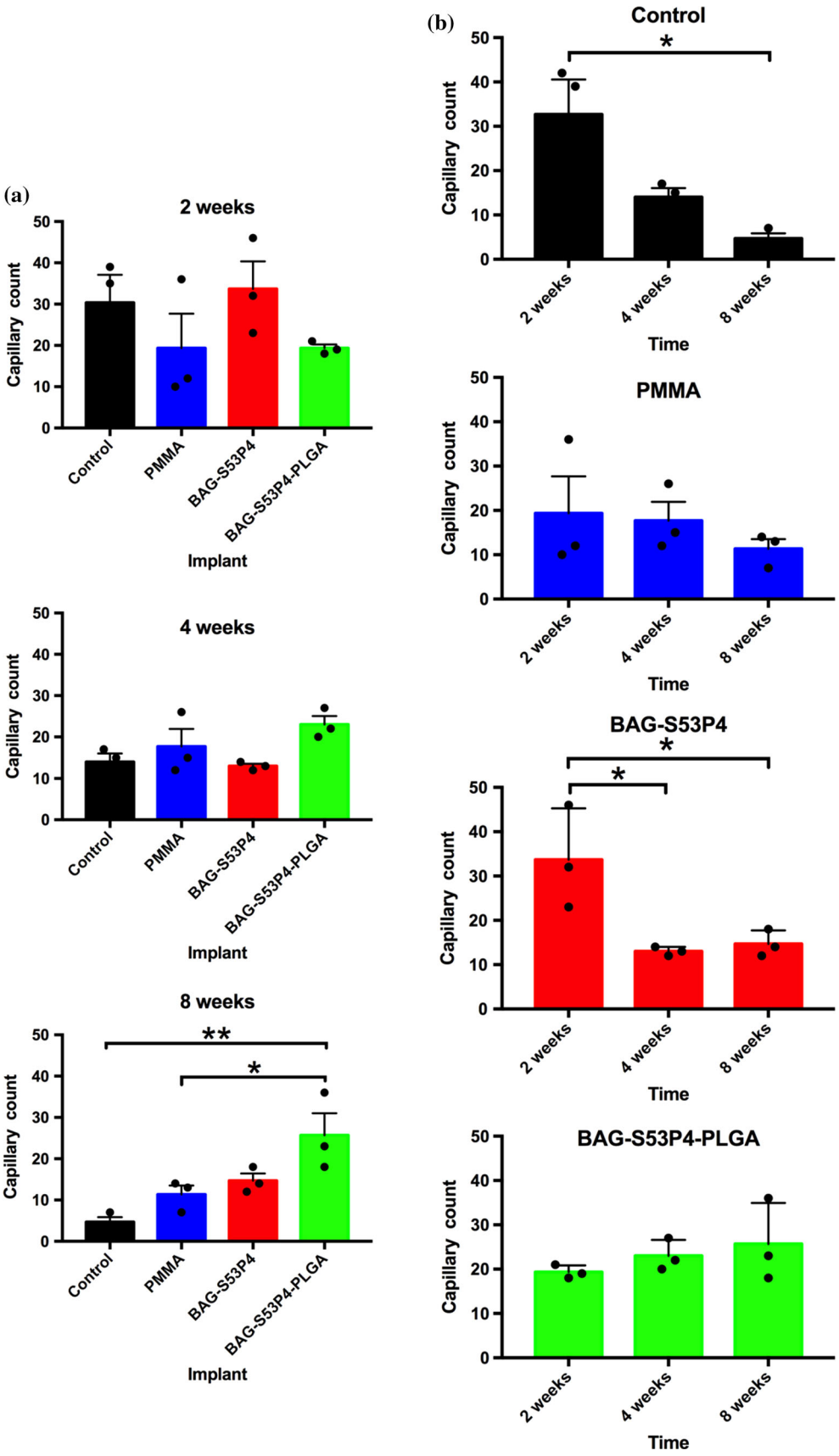
(a)
2 weeks
Capillary count
Control
PMMA
BAG-S53P4
BAG-S53P4-PLGA
Implant
4 weeks
8 weeks
**
*
(b)
Control
PMMA
BAG-S53P4
BAG-S53P4-PLGA
2 weeks
4 weeks
8 weeks
Time

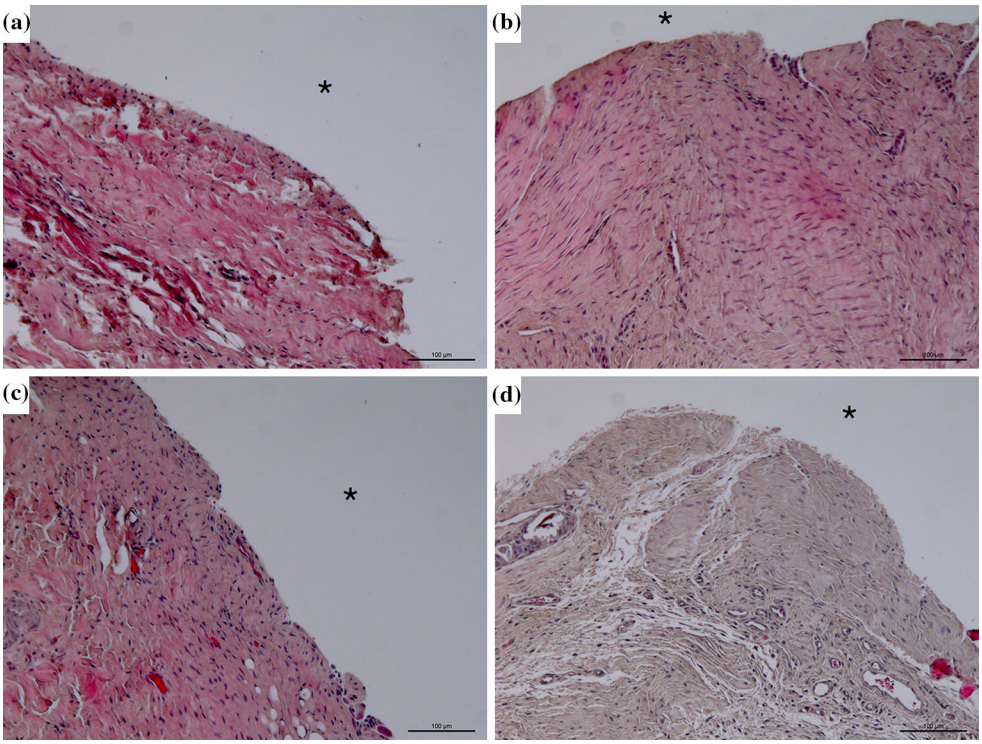

Figure 4 Histology demonstrating capillary beds of the induced membrane formed at 8 weeks on BAG-S53P4-PLGA, BAG-S53P4 and PMMA implants and the negative control. *Scale bar* is set to 100 μm. The *asterisk* indicates the surface against implant. **a** Control. **b** PMMA. **c** BAG-S53P4. **d** BAG-S53P4-PLGA.

Discussion

We evaluated the pro-angiogenetic activity as VEGF expression in an induced membrane formed on the soft tissue interface of BAG-S53P4 and PLGA-coated BAG-S53P4 rods in comparison with PMMA, the gold standard material used in the two-stage induced-membrane technique. Of the combinations of materials tested, only the BAG-S53P4-PLGA-induced membrane showed a continuous increase in VEGF expression, which was observed to be at its highest level at 8 weeks. To our knowledge, a similar continuous increase in VEGF expression has not been reported earlier. During the same time period, the VEGF expression of the PMMA-induced membrane decreased constantly, in concordance with observations in a comparable study in humans [5] as well as in an in vivo rabbit study [6].

The pro-angiogenetic potential that we observed for BAGs, i.e., the increase in VEGF expression, is consistent with several previous in vitro and in vivo studies [11–13]. Particles of BAG-45S5 and BAG-S53P4 have been shown to increase VEGF secretion from human fibroblast cells in a size- and concentration-dependent manner. For BAG-S54P4, an enhanced VEGF release was observed for particles of both 0.5–0.8 and 1–2 mm size, whereas a particle size of 2–3.15 mm led to an inhibition of VEGF release [13]. Fibroblasts stimulated with BAG-S45S5 particles are known to increase proliferation of human dermal microvascular endothelial cells and enhance neovascularization [14]. BAG-S45S5 has also been found to increase the pro-angiogenetic properties of degradable polymers. PLGA spheres containing 10% (w/v) BAG-45S5 particles have been demonstrated to stimulate an increase in VEGF by fibroblasts [15]. Compared with pure poly(D,L-lactide) PDLLA, an addition of BAG to a PDLLA matrix also stimulated angiogenic signaling in fibroblasts by increasing VEGF secretion in a dose-dependent manner.

It is not known how PLGA coating of BAGs affects VEGF expression in an induced membrane. In general, it is, however, known that coating BAGs with a biodegradable polymer decreases the dissolution rate of the glass [16]. The expression pattern in the induced membrane may be explained as follows: According to the expected chemical reactions at the PLGA-coated BAG-S53P4 surface, the polymer will

degrade, subsequently increasing the angiogenic potential of the BAG. Simultaneously with the degradation of the polymer, the surface reactions at the BAG will occur as a continuous release of Ca, Na, P and Si from the BAG in solution has been demonstrated to occur after implantation, thus continuing the increase in VEGF expression observed for BAGs [17].

The higher VEFG expression of the BAG-S53P4-induced membrane compared to the BAG-S53P4-PLGA-induced membrane at 2 weeks suggests that the ions released from BAG-S53P4 positively affect the VEGF expression and that the polymer effectively slows down the ion release and the gene expression. This retarding effect can depend on the polymer barrier preventing contact with the uncoated part of the BAG-S53P4 scaffold or the ability of the polymer degradation products to neutralize the interfacial solution and thus slow down the ion release rate from the glass. At prolonged implantation, the polymer will partly degrade allowing a higher ion release from the BAG-S53P4-based structure. This implies that the partly polymer-coated scaffold enables a continuous release of ions over a longer period of time at concentrations high enough to support VEGF expression than the uncoated scaffold.

The Ca^{2+} ion is known to play a significant role in the VEGF-regulated multifunctional signaling pathway [2], which is known to influence the mobilization of Ca^{2+}. Bone marrow-derived progenitor cells, important in angiogenesis, have been demonstrated to respond to changes in extracellular calcium, through a calcium-sensing receptor as well. The high VEGF expression for both BAG-S53P4 and BAG-S53P4-PLGA may depend on the ion release of Ca^{2+}, which takes place at the surface of the glass. Scaffolds with incorporated BAGs have also been demonstrated to stimulate neovascularization. The mechanisms are unknown, but they are thought to depend on the Ca^{2+} ion release at the glass surface. The increase in VEGF secretion from human fibroblast cells induced by BAG-S53P4 has also been demonstrated to depend on the size of the reacting glass granules, in favor of smaller particles. This may be explained by higher concentrations of ions released from the smaller particles possessing a higher surface area to solution volume ratio, influencing the dissolution process of the glass.

In 1970, Carlisle showed that silicon affects bone growth by demonstrating disturbed bone formation in silicon-deprived chicken. It has been postulated that silicon also may affect angiogenesis and neovascularization. Akermanite ($Ca_2MgSi_2O_7$), a silicate bioceramic, has been demonstrated to cause Si-ion-stimulated proliferation of human aortic endothelial cells. A more rapid increase in blood vessel containing Haversian and Volkmann's canals has been observed for akermanite in comparison with tricalciumphosphate implants in vivo, indicating that silicon may affect neovascularization [18]. A bioactive material only containing silicon and calcium has also been demonstrated to stimulate angiogenesis in a fibroblast and endothelial cell culture, and thus, it has been postulated that silicon may play an important role in initiating angiogenesis [19]. However, in both of the previously mentioned studies, the materials also consisted of calcium, which affects angiogenesis.

Also contradictory pro-angiogenetic observations for silicon have been reported. Silica nanoparticles (SiNPs) have been demonstrated to disturb endothelial cell homeostasis and to impair angiogenesis due to enhanced autophagic activity. SiNPs seem to have an inhibitory effect on angiogenesis on zebrafish via a down-regulation of the VEGF2/Erk1/2 signaling pathway [20]. Mesoporous silica nanospheres have been reported not to have on obvious effect on VEGF stimulation of human bone marrow stromal cells [21]. These anti-angiogenetic findings may, however, be dependent of the size of the particles.

In a study on the response of osteoblast-like cells to 17 metals, an excellent cell proliferation and a high ability to affect collagen synthesis have been observed for silicon [22]. It is known that silicon deprivation decreases collagen formation in bone and it has also been suggested that silicon plays an important role in wound healing. As blood vessels contain collagen, it can thus be speculated that silicon may play an important part in neovascularization due to its relevance in collagen formation and perhaps a lesser part in VEGF stimulation.

In the induced-membrane technique, the second operation is usually performed between 4 and 8 weeks after the first procedure, but it has been speculated that the optimal time for performing the second-stage surgery may be within a month after implantation of PMMA. This is based on histological observations showing that the vascularization in PMMA-induced membranes is ample in one-month-old samples and decreases to less than 60% in three-

month-old samples [5]. This finding is supported by our study, as the inductive capacity of PMMA on VEGF expression seems to be lowest at 8 weeks, the time when many operations are performed. In our study, the PMMA-induced membranes and membranes of the control drill showed their highest capillary density at 2 weeks, with a decreasing trend during follow-up, compared with the BAG-induced membranes, which showed high capillary density throughout the follow-up.

Fracture healing and bone regeneration are complex processes that involve coordinated interplay between the cells of the innate immune system and various osteoprogenitor cells [22, 23]. Fracture healing is initiated by an acute inflammation characterized by production of pro-inflammatory cytokines, e.g., TNF that regulate the recruitment and differentiation of mesenchymal stem cells along the chondrogenic and osteogenic lineages. Indeed, a short period of TNF production is crucial for bone regeneration. In the subsequent state of fracture healing, ingrowth of vasculature in the fracture site is crucial for the bone regeneration. This angiogenesis is mediated by growth factors such as VEGF. Thus, both TNF and VEGF have been shown to play a key role in the various stages of bone regeneration [22, 23].

The expression of TNF for PMMA constantly decreased during the 8-week period, in accordance with previously described observations of low VEGF expression for PMMA. For BAG-S53P4, which clinically is known to be a well-tolerated bone substitute without observed inflammatory response, an increase in TNF expression was observed at 4 weeks.

A limitation of the study is that it focuses on comparison of inflammatory and angiogenic responses elicited by the materials, while the osteogenic potential of the induced membranes was not evaluated. Additionally, the sample size per group is small, and thus, the results need to be interpreted cautiously.

In summary, our study reveals that both uncoated and coated porous BAG-S53P4 implants positively affect the expression of VEGF and TNF, resulting in higher amounts of capillary beds observed in histological samples, compared with the lower expression of VEGF and less capillary beads observed in control and PMMA samples.

The induced membrane of PMMA is known to have angiogenetic-improving properties, which, however, appear to decrease over time. In the induced membrane of PLGA-coated BAG-S53P4, we observed an inductive expression of VEGF that increased with time. At 8 weeks, the expression of VEGF was significantly higher for coated BAG-S53P4 than for PMMA ($p < 0.036$). PLGA-coated BAG-S53P4 is thus an attractive biomaterial for further development of a one-stage induced-membrane technique, as the composite material carries both angiogenic and osteoregenerative properties.

Compliance with ethical standards

Conflict of interest All authors certify that there is no conflict of interest regarding this study.

References

[1] Atique FB, Khalil MM (2014) The bacterial contamination of allogenic bone emergence of multidrug-resistant bacteria in tissue bank. Biomed Res Int Article ID 430581:1–5

[2] Zacchary I (2003) VEGF signaling: integration and multitasking in endothelial cell biology. Biochem Soc Trans 31:1171–1177

[3] Keramaris NC, Calori GM, Nikolaou VS, Schemitsch EH, Giannoudis PV (2008) Fracture vascularity and bone healing: a systematic review of the role of VEGF. Injury 39(S2):45–57

[4] Masquelet AC, Fitoussi F, Begue T (2000) Reconstruction of the long bones by the induced membrane and spongy autograft. Orthop Clin North Am 41:27–37

[5] Aho O-A, Lehenkari P, Ristiniemi J, Lehtonen S, Risteli J, Leskelä H-L (2013) The mechanism of action of induced membranes in bone repair. J Bone Joint Surg 95:597–604

[6] Pelissier PH, Masquelet AC, Bareile R, Pelissier SM, Amedee J (2004) Induced membranes secrete growth factors including vascular and osteoinductive factors and could stimulate bone regeneration. J Orthop Res 22:73–79

[7] Hench LL, Paschall HA (1973) Direct chemical bond of bioactive glass–ceramic materials to bone and muscle. J Biomed Mater Res Symp 4:25–42

[8] Hench LL (2006) The story of bioglass. J Mater Sci Mater Med 17:967–978

[9] Zhang D, Leppäranta O, Munukka E, Ylänen H, Viljanen MK, Eerola E, Hupa M, Hupa L (2010) Antibacterial effects and dissolution behavior of six bioactive glasses. J Biomed Mater Res 93A(2):475–483

[10] Munukka E, Leppäranta O, Korkeamäki M, Vaahto M, Peltola T, Zhang D, Hupa L, Ylänen H, Salonen JI, Viljanen MK, Eerola E (2008) Bactericidal effects of bioactive glasses

on clinically important aerobic bacteria. J Mater Sci Mater Med 19:27–32

[11] Gorustovich A, Roether J, Boccaccini A (2010) Effect of bioactive glasses on angiogenesis: a review of in vitro and in vivo evidences. Tissue Eng B Rev 16(2):199–207

[12] Gerhardt L-C, Widdows KL, Erol MM, Burch CW, Sanz-Herrera J, Ochoa I, Stämpfli R et al (2011) The pro-angiogenic properties of multi-functional bioactive glass composite scaffolds. Biomaterials 32(17):4096–4108

[13] Detsch R, Storr P, Grűnewald A, Roether JA, Lindfors NC, Boccaccini AR (2014) Increase in VEGF secretion from human fibroblast cells by bioactive glass S53P4 to stimulate angiogenesis in bone. J Biomed Mater Res 102A:4055–4061

[14] Day D (2005) Bioactive glass stimulates the secretion of angiogenic growth factors and angiogenesis in vitro. Tissue Eng 11:768–778

[15] Keshaw H, Forbes A, Day RM (2005) Release of angiogenic growth factors from cells encapsulated in alginate beads with bioactive glass. Biomaterials 26(19):4171–4179

[16] Erol M, Özyuguran A, Özarpat Ö, Kucukbayrak S (2012) 3D composite scaffolds using strontium containing bioactive glasses. J Eur Ceram Soc 32:2747–2755

[17] Fagerlund S, Ek P, Hupa L, Hupa M (2012) Dissolution kinetics of a bioactive glass by continuous measurement. J Am Ceram Soc:1–8

[18] Zhai W, Lu H, Chen L, Lin X, Huang Y, Dai K, Naoki K, Chen G, Chang J (2012) Silicate bioceramics induce angiogenesis during bone regeneration. Acta Biomater 8:341–349

[19] Li H, Chang J (2013) Bioactive silicate materials stimulate angiogenesis in fibroblast and endothelial cell co-culture system through paracrine effect. Acta Biomater 9:6981–6991

[20] Duan J, Yu Y, Yu Y, Li Y, Huang P, Zhou Z, Peng S, Sun Z (2014) Silica nanoparticles enhance autophagic activity, disturb endothelial cell homeostasis and impair angiogenesis. Int J Nanomed 9:5131–5141

[21] Shi M, Zhou Y, Shao J, Chen Z, Song B, Chang J, Wu C, Xiao Y (2015) Stimulation of osteogenesis and angiogenesis of hBMSCs by delivering Si ions and functional drug from mesoporous silica nanospheres. Acta Biomater 21:178–189

[22] Zhang D, Wong CS, Wen C, Li Y (2016) Cellular responses of osteoblast-like cells to 17 elemental metals. J Biomed Mater Res A. doi:10.1002/jbm.a.35895

[23] Claes L, Recknagel S, Ignatius A (2012) Fracture healing under healthy and inflammatory conditions. Nat Rev Rheumatol 8(3):133–143. doi:10.1038/nrrheum.2012.1

[24] Loi F, Córdova LA, Pajarinen J, Lin TH, Yao Z, Goodman SB (2016) Inflammation, fracture and bone repair. Bone 86:119–130